

**HYDROGEN PRODUCTION FROM WATER SPLITTING UNDER UV  
LIGHT IRRADIATION OVER Cu-LOADED MESOPOROUS-ASSEMBLED  
SrTi<sub>x</sub>Zr<sub>1-x</sub>O<sub>3</sub> AND SrTi<sub>x</sub>Si<sub>1-x</sub>O<sub>3</sub> NANOCRYSTAL PHOTOCATALYSTS**



Pusratha Wongchanapai

A Thesis Submitted in Partial Fulfilment of the Requirements  
for the Degree of Master of Science  
The Petroleum and Petrochemical College, Chulalongkorn University  
in Academic Partnership with  
The University of Michigan, The University of Oklahoma,  
Case Western Reserve University, and Institut Français du Pétrole  
2012

551757

**Thesis Title:** Hydrogen Production from Water Splitting under UV Light Irradiation over Cu-Loaded Mesoporous-Assembled  $\text{SrTi}_x\text{Zr}_{1-x}\text{O}_3$  and  $\text{SrTi}_x\text{Si}_{1-x}\text{O}_3$  Nanocrystal Photocatalysts

**By:** Pusratha Wongchanapai

**Program:** Petrochemical Technology

**Thesis Advisors:** Prof. Sumaeth Chavadej  
Assoc. Prof. Pramoch Rangsunvigit

---

Accepted by The Petroleum and Petrochemical College, Chulalongkorn University, in partial fulfilment of the requirements for the Degree of Master of Science.

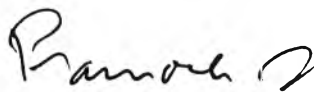


..... College Dean  
(Asst. Prof. Pomthong Malakul)

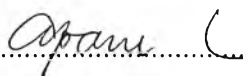
**Thesis Committee:**



.....  
(Prof. Sumaeth Chavadej)



.....  
(Assoc. Prof. Pramoch Rangsunvigit)



.....  
(Assoc. Prof. Apanee Leungnaruemitchai)



.....  
(Dr. Tarawipa Puangpetch)

## ABSTRACT

5371035063: Petrochemical Technology Program

Pusratha Wongchanapai: Hydrogen Production from Water Splitting under UV Light Irradiation over Cu-Loaded Mesoporous-Assembled  $\text{SrTi}_x\text{Zr}_{1-x}\text{O}_3$  and  $\text{SrTi}_x\text{Si}_{1-x}\text{O}_3$  Nanocrystal Photocatalysts

Thesis Advisors: Prof. Sumaeth Chavadej, and Assoc. Prof. Pramoch Rangsunvigit 85 pp.

Keywords: Hydrogen production/ Mesoporous material / Perovskite/ Photocatalysis/ Water splitting

Nowadays, the global demand for energy is expected to increase, and the primary source of currently consumed energy is fossil fuels, e.g. petroleum oils, which cause global warming because fossil fuels produce a large amount of  $\text{CO}_2$ . So, renewable and environmentally friendly energy resources are desirable and have tendency to increase in the future. Hydrogen has received great attention for use as an alternative and renewable energy source for internal-combustion engines and fuel cells. Photocatalytic water splitting can produce hydrogen by using solar light as an energy source and water as a feedstock.  $\text{SrTiO}_3$  is one of the interesting photocatalysts due to its superior physicochemical properties, such as its excellent thermal stability, photocorrosion resistibility, and good structure stability as the host for metal ion doping. The purpose of this work was to optimize the composition of mesoporous-assembled  $\text{SrTi}_x\text{Zr}_{1-x}\text{O}_3$  and  $\text{SrTi}_x\text{Si}_{1-x}\text{O}_3$  nanocrystals, which were synthesized by a sol-gel process with the aid of a structure-directing surfactant for achieving the highest photocatalytic activity for hydrogen production from water splitting under UV light irradiation with methanol as a hole scavenger. The mesoporous-assembled  $\text{SrTi}_{0.93}\text{Zr}_{0.07}\text{O}_3$  and  $\text{SrTi}_{0.95}\text{Si}_{0.05}\text{O}_3$  photocatalysts calcined at  $700\text{ }^\circ\text{C}$  were found to show the better the photocatalytic hydrogen production activity than the other  $\text{SrTi}_x\text{Zr}_{1-x}\text{O}_3$  and  $\text{SrTi}_x\text{Si}_{1-x}\text{O}_3$  photocatalysts. Moreover, the Cu loadings by photochemical deposition method were found to greatly enhance the photocatalytic activity of the  $\text{SrTi}_{0.93}\text{Zr}_{0.07}\text{O}_3$  and  $\text{SrTi}_{0.95}\text{Si}_{0.05}\text{O}_3$  photocatalysts.

## บทคัดย่อ

กัศรัฐฐา วงศ์ชนะภัย: การผลิตไฮโดรเจนจากโมเลกุลของน้ำภายใต้สภาวะที่มีแสงโดยใช้ตัวเร่งปฏิกิริยาสทอนเทียมไททานเนียมเซอร์โคเนตและสทอนเทียมไททานเนียมซิลิเกตที่มีขนาดอนุภาคเล็กและรูพรุนในระดับนาโนเมตรซึ่งถูกกระตุ้นด้วยคอปเปอร์ (Hydrogen Production from Water Splitting under UV Light Irradiation over Cu-Loaded Mesoporous-Assembled  $\text{SrTi}_x\text{Zr}_{1-x}\text{O}_3$  and  $\text{SrTi}_x\text{Si}_{1-x}\text{O}_3$  Nanocrystal Photocatalysts) อ. ที่ปรึกษา : ศ. ดร. สุเมธ ชวเดช และ รศ. ดร. ปราโมช รังสรรค์วิจิตร 85 หน้า

ในปัจจุบันความต้องการในการใช้พลังงานเพิ่มมากขึ้น และพลังงานที่สำคัญ คือ เชื้อเพลิงธรรมชาติ ได้แก่ น้ำมันปิโตรเลียมและถ่านหิน ซึ่งเป็นสาเหตุที่ทำให้เกิดภาวะโลกร้อน เพราะเชื้อเพลิงธรรมชาติทำให้เกิดก๊าซคาร์บอนไดออกไซด์เป็นจำนวนมาก ไฮโดรเจนได้รับความสนใจอย่างมากเพื่อใช้เป็นพลังงานทางเลือกใหม่และพลังงานทดแทนสำหรับรถยนต์และเซลล์เชื้อเพลิง ไฮโดรเจนสามารถถูกผลิตได้จากแหล่งพลังงานที่สามารถหาได้อย่างไม่จำกัด ได้แก่ น้ำ และแสงอาทิตย์ พร้อมกับตัวเร่งปฏิกิริยาแบบใช้แสงร่วมที่เหมาะสมเป็นตัวช่วยให้เกิดปฏิกิริยา ตัวเร่งปฏิกิริยาสทอนเทียมไททานเนตได้รับความสนใจเนื่องจากมีคุณสมบัติทางกายภาพและทางเคมีที่เหมาะสม เช่น มีความเสถียรต่ออุณหภูมิ, มีด้านทานต่อการกัดกร่อน และมีโครงสร้างที่เสถียรสามารถได้ไปโลหะอื่นๆ ลงไปได้ ในงานวิจัยนี้มุ่งเน้นศึกษาการปรับปรุงและพัฒนาความสามารถในการผลิตไฮโดรเจนของตัวเร่งปฏิกิริยาแบบใช้แสงร่วมสทอนเทียมไททานเนียมเซอร์โคเนตและสทอนเทียมไททานเนียมซิลิเกตที่มีขนาดอนุภาคเล็กและรูพรุนในระดับนาโนเมตร ในการทดลองนี้ตัวเร่งปฏิกิริยาแบบใช้แสงร่วมถูกสังเคราะห์ขึ้น โดยกระบวนการโซล-เจลร่วมกับการใช้สารลดแรงตึงผิวเป็นตัวกำหนดโครงสร้าง จากผลการทดลองพบว่าตัวเร่งปฏิกิริยาแบบใช้แสงร่วมสทอนเทียมไททานเนียมเซอร์โคเนตและสทอนเทียมไททานเนียมซิลิเกต ที่ประกอบด้วยอัตราส่วนของไททานเนียมและเซอร์โคเนียมเท่ากับ 0.93:0.07 และอัตราส่วนของไททานเนียมและซิลิกอนเท่ากับ 0.95:0.05 ตามลำดับ ซึ่งถูกเผาที่อุณหภูมิ 700 องศาเซลเซียส ให้ผลในการผลิตไฮโดรเจนดีกว่าตัวเร่งปฏิกิริยาสทอนเทียมไททานเนียมเซอร์โคเนตและสทอนเทียมไททานเนียมซิลิเกตตัวอื่น การใส่คอปเปอร์แบบใช้แสงร่วมด้วยวิธีการยัดเกาะด้วยกระบวนการเคมีในปริมาณที่เหมาะสมบนตัวเร่งปฏิกิริยาดังกล่าวพบว่า อัตราการเกิดไฮโดรเจนมีค่าเพิ่มขึ้น

## ACKNOWLEDGEMENTS

This thesis work is funded by the Petroleum and Petrochemical College, and by the Center of Excellence on Petrochemical and Materials Technology, Thailand.

The author would like to express her sincere gratitude to Prof. Sumaeth Chavadej and Assoc. Prof. Pramoch Rangsunvigit for their invaluable guidance, understanding, and constant encouragement throughout the course of this research.

She would like to express special thanks to Assoc. Prof. Apanee Leungnaruemitchai and Dr. Tarawipa Puangpetch for kindly serving on her thesis committee. Their sincere suggestions are definitely imperative for accomplishing her thesis.

Her gratitude is absolutely extended to all staffs of the Petroleum and Petrochemical College, Chulalongkorn University, for all their kind assistance and cooperation.

Furthermore, she would like to take this important opportunity to thank all of her graduate friends for their unforgettable friendship.

Finally, she really would like to express her sincere gratitude to her parents and family for the love, understanding, and cheering.

## TABLE OF CONTENTS

	<b>PAGE</b>
Title Page	i
Abstract (in English)	iii
Abstract (in Thai)	iv
Acknowledgements	v
Table of Contents	vi
List of Tables	ix
List of Figures	x
<b>CHAPTER</b>	
<b>I INTRODUCTION</b>	<b>1</b>
<b>II LITERATURE REVIEW</b>	<b>4</b>
2.1 Hydrogen: Fuel of the Future	4
2.2 Water Splitting: Hydrogen Generation Using Solar Energy	5
2.2.1 Photocatalytic Reaction	5
2.2.2 Splitting Water into Hydrogen	7
2.2.3 Efficiency	9
2.2.4 Semiconductor	9
2.2.5 Types of Semiconductor Systems Proposed for Solar Water Splitting	11
2.2.5.1 Semiconductor Solid State Photovoltaic Based Systems	11
2.2.5.2 Semiconductor Electrode Systems	12
2.2.5.3 Semiconductor Particle Systems	13
2.2.6 The Principle of Water Splitting Using Semiconductor Particle	14
2.3 Photocatalyst	16

<b>CHAPTER</b>	<b>PAGE</b>
2.4. Titanium Oxide Photocatalyst	17
2.4.1 General Remarks	17
2.4.2 Crystal Structure and Properties	18
2.4.3 Semiconductor Characteristic and Photocatalytic Activity	20
2.5 Nano-Photocatalyst	22
2.5.1 General Remarks	22
2.5.2 Activity of Nano-Photocatalyst	22
2.6 Chemical Additive for Enhancement of Photocatalytic H <sub>2</sub> Production	24
2.7 Metal Loading for Enhancement of H <sub>2</sub> Production	26
2.8 Mixed Oxide System	27
2.9 Porous Material	30
2.10 Sol-Gel Process	31
 <b>III EXPERIMENTAL</b>	 35
3.1 Materials and equipment	35
3.1.1 Chemicals	35
3.1.2 Equipment	35
3.2 Methodology	36
3.2.1 Mesoporous-Assembled SrTi <sub>x</sub> Zr <sub>1-x</sub> O <sub>3</sub> and SrTi <sub>x</sub> Si <sub>1-x</sub> O <sub>3</sub> Nanocrystal Photocatalyst Synthesis by a Sol-Gel Process with the Aid of a Structure-Directing Surfactant	37
3.2.2 Photocatalyst Characterizations	39
3.2.3 Photocatalytic H <sub>2</sub> Production System	41
 <b>IV RESULTS AND DISCUSSION</b>	 43
4.1 Photocatalyst Characterization Results	43
4.1.1 TG–DTA Results	43

<b>CHAPTER</b>	<b>PAGE</b>
4.1.2 N <sub>2</sub> Adsorption-Desorption Results	47
4.1.3 XRD Results	52
4.1.4 UV-Visible Spectroscopy Results	58
4.1.5 SEM-EDX Results	63
4.1.6 TEM-EDX Results	67
4.1.7 Hydrogen Chemisorption Results	71
4.2 Photocatalytic Hydrogen Production Activity	72
4.2.1 Effect of Ti-to-Zr and Ti-to-Si Molar Ratio	72
4.2.2 Effect of Calcination Temperature	73
4.2.3 Effect of Cu Loadings	74
<b>V CONCLUSIONS AND RECOMMENDATIONS</b>	<b>77</b>
5.1 Conclusions	77
5.2 Recommendations	77
<b>REFERENCES</b>	<b>78</b>
<b>CURRICULUM VITAE</b>	<b>85</b>



## LIST OF TABLES

TABLE	PAGE
2.1 The band gap positions of some common semiconductor photocatalysts	11
2.2 Definitions about porous solids	30
4.1 Thermal decomposition behavior results of the dried synthesized SrTiO <sub>3</sub> , SrZrO <sub>3</sub> , SrSiO <sub>3</sub> , SrTi <sub>0.93</sub> Zr <sub>0.07</sub> O <sub>3</sub> and SrTi <sub>0.95</sub> Si <sub>0.05</sub> O <sub>3</sub> photocatalysts from TG–DTA analysis	46
4.2 N <sub>2</sub> adsorption-desorption results of the synthesized mesoporous-assembled SrTi <sub>x</sub> Zr <sub>1-x</sub> O <sub>3</sub> and SrTi <sub>x</sub> Si <sub>1-x</sub> O <sub>3</sub> photocatalysts	51
4.3 N <sub>2</sub> adsorption-desorption results of the synthesized Cu-loaded mesoporous-assembled SrTi <sub>0.93</sub> Zr <sub>0.07</sub> O <sub>3</sub> and SrTi <sub>0.95</sub> Si <sub>0.05</sub> O <sub>3</sub> photocatalysts	52
4.4 Summary of XRD analysis of the synthesized mesoporous-assembled SrTi <sub>0.93</sub> Zr <sub>0.07</sub> O <sub>3</sub> and SrTi <sub>0.95</sub> Si <sub>0.05</sub> O <sub>3</sub> photocatalysts	57
4.5 Summary of XRD analysis of the synthesized Cu-loaded mesoporous-assembled SrTi <sub>0.93</sub> Zr <sub>0.07</sub> O <sub>3</sub> and SrTi <sub>0.95</sub> Si <sub>0.05</sub> O <sub>3</sub> photocatalysts	58
4.6 Absorption onset wavelength and band gap energy results of the synthesized mesoporous-assembled SrTi <sub>x</sub> Zr <sub>1-x</sub> O <sub>3</sub> , SrTi <sub>x</sub> Si <sub>1-x</sub> O <sub>3</sub> photocatalysts without and with Cu loadings and calcined at various temperatures	62
4.7 Cu dispersion results over the Cu-loaded mesoporous-assembled SrTi <sub>0.93</sub> Zr <sub>0.07</sub> O <sub>3</sub> , and SrTi <sub>0.95</sub> Si <sub>0.05</sub> O <sub>3</sub> photocatalysts calcined at 700 °C	71

## LIST OF FIGURES

FIGURE	PAGE	
2.1	Relative emissions of greenhouse gases (expressed in carbon units per km) for vehicles powered by today's internal combustion engine using gasoline compared to vehicles powered by fuel cells.	5
2.2	Types of photocatalytic reactions: (a) photoinduced reaction and (b) photon energy conversion reaction.	6
2.3	Electrochemical cell, in which a TiO <sub>2</sub> electrode is connected with a Pt electrode.	8
2.4	The structure of band gap energy.	10
2.5	Schematic of (a) solid state photovoltaic cell driving a water electrolyzer and (b) cell with immersed semiconductor p/n junction (or metal/semiconductor Schottky junction) as one electrode.	12
2.6	Schematic of liquid junction semiconductor electrode cell.	13
2.7	Representation of semiconductor particulate systems for heterogeneous photocatalysis.	14
2.8	Reaction schematic for water splitting reaction over semiconductor photocatalysts.	15
2.9	Processes occurring in semiconductor photocatalyst under photoexcitation for water splitting reaction.	16
2.10	Band gap energy of the photocatalyst.	17
2.11	Crystal structures of (a) anatase, (b) rutile, and (c) brookite.	18
2.12	Photocatalytic hydrogen production over anatase/rutile TiO <sub>2</sub> under the mediation of I <sup>-</sup> /IO <sub>3</sub> <sup>-</sup> .	25
2.13	A schematic of forming the BaTiO <sub>3</sub> nanoparticles.	33
3.1	Synthesis procedure for mesoporous-assembled SrTi <sub>x</sub> Zr <sub>1-x</sub> O <sub>3</sub> and SrTi <sub>x</sub> Si <sub>1-x</sub> O <sub>3</sub> photocatalysts: (a) without and (b) with Cu loading by PCD method.	38

<b>FIGURE</b>	<b>PAGE</b>
3.2 Setup of photocatalytic H <sub>2</sub> production system.	42
4.1 TG-DTA curves of the dried synthesized (a) SrTiO <sub>3</sub> , (b) SrZrO <sub>3</sub> , (c) SrSiO <sub>3</sub> , (d) SrTi <sub>0.93</sub> Zr <sub>0.07</sub> O <sub>3</sub> and (e) SrTi <sub>0.95</sub> Si <sub>0.05</sub> O <sub>3</sub> photocatalysts.	44
4.2 N <sub>2</sub> adsorption-desorption isotherms and pore size distributions (inset) of the synthesized (a) SrTiO <sub>3</sub> , (b) SrTi <sub>0.93</sub> Zr <sub>0.07</sub> O <sub>3</sub> , (c) SrTi <sub>0.95</sub> Si <sub>0.05</sub> O <sub>3</sub> , (d) 0.25 wt.% Cu loaded SrTi <sub>0.93</sub> Zr <sub>0.07</sub> O <sub>3</sub> , and (e) 0.75 wt.% Cu loaded SrTi <sub>0.95</sub> Si <sub>0.05</sub> O <sub>3</sub> photocatalysts calcined at 700 °C.	48
4.3 XRD patterns of the synthesized (a) SrTi <sub>x</sub> Zr <sub>1-x</sub> O <sub>3</sub> and (b) SrTi <sub>x</sub> Si <sub>1-x</sub> O <sub>3</sub> photocatalysts calcined at 700 °C for 4 h.	54
4.4 XRD patterns of the synthesized SrTi <sub>0.95</sub> Si <sub>0.05</sub> O <sub>3</sub> photocatalysts calcined at various temperatures for 4 h.	55
4.5 XRD patterns of the Cu-loaded synthesized (a) SrTi <sub>0.93</sub> Zr <sub>0.07</sub> O <sub>3</sub> and (b) SrTi <sub>0.95</sub> Si <sub>0.05</sub> O <sub>3</sub> photocatalysts with various Cu loadings calcined at 700°C for 4 h.	56
4.6 UV-visible spectra of the synthesized mesoporous-assembled photocatalysts calcined at 700 °C: (a) SrTiO <sub>3</sub> and (b)-(f) SrTi <sub>x</sub> Zr <sub>1-x</sub> O <sub>3</sub> .	60
4.7 UV-visible spectra of the synthesized mesoporous-assembled photocatalysts calcined at 700 °C: (a) SrTiO <sub>3</sub> and (b)-(f) SrTi <sub>x</sub> Si <sub>1-x</sub> O <sub>3</sub> .	60
4.8 UV-visible spectra of the synthesized mesoporous-assembled SrTi <sub>0.95</sub> Si <sub>0.05</sub> O <sub>3</sub> photocatalysts calcined at various temperatures.	61
4.9 UV-visible spectra of the synthesized mesoporous-assembled photocatalysts calcined at 700 °C: (a) SrTi <sub>0.93</sub> Zr <sub>0.07</sub> O <sub>3</sub> , (b) SrTi <sub>0.95</sub> Si <sub>0.05</sub> O <sub>3</sub> , (c) 1.25 wt.% Cu-loaded SrTi <sub>0.93</sub> Zr <sub>0.07</sub> O <sub>3</sub> , and (d) 0.75 wt.% Cu-loaded SrTi <sub>0.95</sub> Si <sub>0.05</sub> O <sub>3</sub> .	61
4.10 SEM images of the synthesized mesoporous-assembled photocatalysts calcined at 700 °C: (a) SrTi <sub>0.93</sub> Zr <sub>0.07</sub> O <sub>3</sub> , (b) 0.25 wt.% Cu-loaded SrTi <sub>0.93</sub> Zr <sub>0.07</sub> O <sub>3</sub> , (c) SrTi <sub>0.95</sub> Si <sub>0.05</sub> O <sub>3</sub> and (d) 0.75 wt.% Cu-loaded SrTi <sub>0.95</sub> Si <sub>0.05</sub> O <sub>3</sub> .	64

FIGURE	PAGE
4.11 SEM image and EDX area mappings of the synthesized 0.25 wt.% Cu-loaded mesoporous-assembled $\text{SrTi}_{0.93}\text{Zr}_{0.07}\text{O}_3$ photocatalyst calcined at 700 °C.	65
4.12 SEM image and EDX area mappings of the synthesized 0.75 wt.% Cu-loaded mesoporous-assembled $\text{SrTi}_{0.95}\text{Si}_{0.05}\text{O}_3$ photocatalyst calcined at 700 °C.	66
4.13 TEM images of the synthesized mesoporous-assembled photocatalysts calcined at 700 °C: (a) $\text{SrTiO}_3$ , (b) $\text{SrTi}_{0.93}\text{Zr}_{0.07}\text{O}_3$ , and (c) $\text{SrTi}_{0.95}\text{Si}_{0.05}\text{O}_3$ .	68
4.14 TEM image and EDX point mapping of the synthesized 0.25 wt.% Cu-loaded mesoporous-assembled $\text{SrTi}_{0.93}\text{Zr}_{0.07}\text{O}_3$ photocatalyst calcined at 700 °C.	69
4.15 TEM image and EDX point mapping of the synthesized 0.75 wt.% Cu-loaded mesoporous-assembled $\text{SrTi}_{0.95}\text{Si}_{0.05}\text{O}_3$ photocatalyst calcined at 700 °C.	70
4.16 Effect of Ti-to-Zr and Ti-to-Si molar ratio on specific hydrogen production rate over the synthesized mesoporous-assembled $\text{SrTi}_x\text{Zr}_{1-x}\text{O}_3$ and $\text{SrTi}_x\text{Si}_{1-x}\text{O}_3$ photocatalysts calcined at 700 °C.	73
4.17 Effect of calcination temperature on specific hydrogen production rate over the synthesized mesoporous-assembled $\text{SrTi}_{0.95}\text{Si}_{0.05}\text{O}_3$ photocatalysts.	74
4.18 Effect of Cu loading on specific hydrogen production rate over the synthesized mesoporous-assembled $\text{SrTi}_{0.93}\text{Zr}_{0.07}\text{O}_3$ and $\text{SrTi}_{0.95}\text{Si}_{0.05}\text{O}_3$ photocatalysts.	76